Strain Avalanches in Microsized Single Crystals: A Theoretical Study of the Relation between the Avalanche Size and Duration *

Xu Zhang(张旭)[1,2], Zhi Wang(王志)[1], Qian Li(李倩)[1], Fu-Lin Shang(尚福林)[2]**

[1]*National Center for International Joint Research of Micro-nano Moulding Technology, School of Mechanics and Engineering Science, Zhengzhou University, Zhengzhou 450001*

[2]*State Key Laboratory for Strength and Vibration of Mechanical Structures, School of Aerospace, Xi'an Jiaotong University, Xi'an 710049*

(Received 4 May 2016)

Single crystal micropillars deform via a sequence of discrete strain avalanches, observed as displacement jumps or stress drops. Here we develop a simple crystal plasticity model to provide a quantitative expression of the relation between avalanche duration and avalanche size. It is found that the avalanche durations in scale with the averaged avalanche sizes only hold for those larger magnitudes. We show that the theoretical predictions are capable of capturing the essential aspects of scaling behaviors from micro-compression tests.

PACS: 64.60.av, 62.20.fq, 62.20.F– DOI: 10.1088/0256-307X/33/9/096401

The plastic flow of small-scale crystals proceeds as a series of discrete strain avalanches, resulting in a pattern of deformation that is spatially inhomogeneous and intermittent in time.[1,2] Analyses of such strain avalanches reveal that micropillar plasticity exhibits power-law scaling behavior, or scale-free plastic flow.[1,3] For example, the statistical analyses of strain avalanches including avalanche sizes S,[3,4] avalanche durations $T_{\rm b}$[5–7] and avalanche velocity $v_{\rm b}$,[2,8] all display the well-known power-law distributions (with a cut-off). It is apparent that the statistical scaling behaviors of the strain avalanches are the same for small FCC and BCC crystals,[9,10] crystal orientation,[4] crystal size,[10] applied deformation rate,[5,10] and loading modes.[3]

The axial compressions of micron and submicron size crystals have reported that larger avalanche sizes are generally associated with longer avalanche durations.[2,11] Moreover, the statistical distributions of S and $T_{\rm b}$ all follow the powerlaws over several decades.[5,12] Thus, one may speculate whether these two distributions possess the same power-law exponents. Unfortunately, very recent experimental observations and theoretical predictions of $T_{\rm b}$ for microsized single crystals both show that the power-law exponent of $P(T_{\rm b})$ is larger than that of $P(S)$,[5,13,14] e.g., $\alpha \approx 2$ versus $\tau \approx 1.5$,[5,10] $\alpha \approx 1.65$ versus $\tau \approx 1.35$.[13] Here τ and α are the power-law exponents of the distributions $P(S) \propto S^{-\tau}$ and $P(T_{\rm b}) \propto T_{\rm b}^{-\alpha}$, respectively. So far, the statistics of strain avalanches are far from being fully understood.

A quantitative description of the relation between the avalanche duration and avalanche size will facilitate a better understanding of the relation between α and τ. Although both the theoretical and experimental studies provide the evidence that larger S is generally associated with longer $T_{\rm b}$, only a qualitative description of the relation between them has been made to date. Up to now, a quantitative characterization of the relation between S and $T_{\rm b}$ has been lacking.

In this Letter, we investigate the relation between the avalanche duration and avalanche size at room temperature by virtue of a simple crystal plasticity model. An important advantage of this model is that it enables us to derive a quantitative expression of the avalanche duration with respect to the avalanche size (plastic strain). The predicted power-law exponents of avalanche durations can describe the micro-compression observations with reasonable accuracy. We demonstrate that the avalanche durations scaling with averaged avalanche sizes only hold for those larger magnitudes. The analysis tools applied here are complementary to the present experiments and simulations on microplasticty with respect to the statistics of strain avalanches at room temperature.

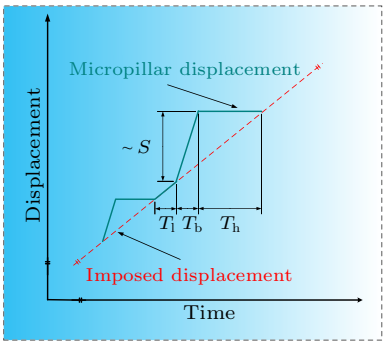

Fig. 1. The schematic plot of micropillar displacements (green) versus time under the HLM, and the dotted line (red) represents the programmed displacement by the nanoindentation system. Within a given avalanche duration $T_{\rm b}$, the burst displacement, which is represented in terms of $\sim S$ in the plot, is MLS, where M is the Schmid factor and L is the length of micropillar. Here $T_{\rm l}$ is a period of loading stage, $T_{\rm h}$ represents the holding time until the imposed displacement captures the micropillar displacement.

To illustrate the avalanche duration and avalanche size explicitly, we first briefly outline the inter-

*Supported by the National Natural Science Foundation of China under Grant No 51404212, the China Postdoctoral Science Foundation under Grant No 2015M572118, and the Basic and Advanced Technology Research Project of Henan Province under Grant No 52110599.

**Corresponding author. Email: shangfl@mail.xjtu.edu.cn

© 2016 Chinese Physical Society and IOP Publishing Ltd

mittent plastic behaviors of quasi-statically deforming micropillars under the hybrid loading method (HLM). Such a method imposes a nominally constant strain rate, except when the micropillar displacement exceeds the imposed displacement by the nanoindentation system, such as during a strain avalanche, whereby the applied load is kept fixed.[15] The schematic diagram of loading process is shown in Fig. 1. The curve portion with the positive slope suggests a higher velocity than that imposed by the nanoindentation system, and thus represents an occurrence of a strain avalanche ($T_{\rm b}$). A horizontal line represents a holding stage ($T_{\rm h}$) and lasts until the actual micropillar displacement reaches the imposed displacement. Following that, a loading stage ($T_{\rm l}$) may occur, associated with the constant strain-rate loading process.

To determine the avalanche duration $T_{\rm b}$, a crystal plasticity model is proposed to produce a series of power-law distributed strain avalanches. It is noteworthy that intermittency has been mostly observed under the single slip conditions.[8,12] In this regard, the present crystal plasticity model represents a two-dimensional (2D) cross section (x–y plane) of a three-dimensional (3D) single crystal with single slip geometry. This may be the case for the investigation of the strain avalanche that is usually dominated by a single slip system in single crystal micropillar plasticity.[4] Since the loading stage of flow intermittency behaviors like the conventional elastic-plastic deformation of bulk crystals, its plastic behaviors can be readily described by the classic crystal plasticity.[16] In the following we only outline the crystal plasticity model that aims to describe the burst deformation.

Whether a burst activity is to be initiated is determined by both a driving force correlated with the externally applied stress $\tau_{\rm ext}$ and a current resistant strength correlated with the internal stress $\tau_{\rm in}$.[2] In this regard, the burst strain rate $\dot{\gamma}(t)$ at time t is phenomenologically assumed to be[16,17]

$$\dot{\gamma}(t) = \dot{\gamma}_0[\tau_{\rm ext}(t)/\tau_{\rm in}(t)]^{1/m}, \tag{1}$$

where m is the rate sensitivity exponent, and $\dot{\gamma}_0$ is the shear rate at a reference condition. In Eq. (1), the evolution of $\tau_{\rm ext}$ is given by

$$\dot{\tau}_{\rm ext}(t) = E \cdot M[\dot{\varepsilon}_0 - M\dot{\gamma}(t)], \tag{2}$$

where E is the elastic modulus, and $\dot{\varepsilon}_0$ is the applied constant strain rate by the nanoindentation system.

We shall mention that the strain burst phenomenon investigated here are limited to the micron and submicron size crystals. Therefore, the evolution of flow strength in the course of plastic deformation is mainly due to the dominance of forest-hardening processes.[18,19] Normally, the phenomenological description of the forest hardening is given by

$$\dot{\tau}_{\rm in}(t) = h(t)\dot{\gamma}(t), \tag{3}$$

where $h(t)$ is the hardening coefficient as a function of t,[16]

$$h(t) = h_0 {\rm sech}^2\Big|\frac{h_0\gamma(t)}{\tau_{\rm s}-\tau_0}\Big|, \quad \gamma(t) = \int_0^t |\dot{\gamma}|dt, \tag{4}$$

where h_0 is the initial hardening modulus, τ_0 is the initial critical resolved shear stress, and $\tau_{\rm s}$ is the saturated shear stress.

Considering the whole strain avalanche, the produced avalanche size S is calculated by[13,17]

$$S = [(1-\xi)\dot{\gamma}^+(t) + \xi\dot{\gamma}^+(t+T_{\rm b+h})]T_{\rm b}, \tag{5}$$

where the superscript + represents the initial strain rate of the present process (strain avalanche or loading stage), ξ is the dimensionless constant and $T_{\rm b+h} = T_{\rm b}+T_{\rm h}$ is the cumulative time duration for the holding stage and burst slip. Considering the displacement-time curve in the micropillar deformation (Fig. 1), $T_{\rm b+h}$ is particularly defined as

$$T_{\rm b+h} = MS/\dot{\varepsilon}_0. \tag{6}$$

Using Eqs. (1)–(6) and the Taylor expansion of $\dot{\gamma}^+(t+T_{\rm b+h})$ in Eq. (5), we obtain the relation between the avalanche duration and avalanche size

$$T_{\rm b}(t,S) = \frac{S}{\dot{\gamma}^+(t)\Big[1+\frac{\xi\Delta\tau_{\rm ex}}{m\tau_{\rm ex}(t)} - \frac{h(t)\xi S}{m\tau_{\rm in}(t)}\Big]}, \tag{7}$$

where $T_{\rm b}(t,S)$ is the function of avalanche size S and the time t at its occurrence. Under the condition of HLM, the applied force is kept fixed during a strain avalanche, thus giving rise to $\Delta\tau_{\rm ex} \approx 0$ in Eq. (7). At applied stress $\tau_{\rm ex} = \tau_{\rm ex}(t)$, Eq. (7) can be rewritten as

$$T_{\rm b}(t,S) = \frac{\tau_{\rm in}(t)mS}{\dot{\gamma}^+(t)[\tau_{\rm in}(t)m - h(t)\xi S]}. \tag{8}$$

This equation provides a quantitative description of the relation between $T_{\rm b}$ and S under the condition of HLM. In Eq. (8), the avalanche size S follows a statistical distribution with a cut-off[4,9]

$$P(S) \sim S^{-\tau}\exp[-(S/S_{\rm max})^2], \tag{9}$$

where $S_{\rm max}$ is an exponential cut-off, which has been discussed in Refs. [4,20,21]. The exponent $\tau = 1.35$ is universal[12] and derived by a recent re-analysis of the experimental micropillar compression data.[20] In this way, S in Eq. (8) could be predicted by using a Monte Carlo stochastic method[13,22] and the generated avalanche sizes in this context will follow the statistical distribution described by Eq. (9).

A quasi-static hybrid loading protocol is implemented as follows: firstly, we increase the applied strain ε from zero with a small increment $\Delta\varepsilon$. After this strain increase, we calculate the stress increment $\Delta\tau_{\rm ext}(\Delta\varepsilon)$ by using Eqs. (1)–(4). Then, we check whether the total applied stress is increased; for example, $\tau_{\rm ext}\cdot\Delta\tau_{\rm ext}(\Delta\varepsilon) > 0$. If it occurs, then we increase the total external stress by $\Delta\tau_{\rm ext}(\Delta\varepsilon)$. If not, a burst slip occurs, and the total external stress keeps constant with $\Delta\tau_{\rm ext}(\Delta\varepsilon) = 0$. Accordingly, we obtain the avalanche size $S = \Delta\varepsilon/M$. Provided that the external

strain increase $\Delta\varepsilon$ also follows the statistical distribution of Eq. (9), this procedure implements a stochastic crystal plasticity model, and the captured avalanche size is expected to follow the statistical distribution described by Eq. (9). To ensure that the occurrence time of strain avalanche is not related to the magnitude of $\Delta\varepsilon$, the value of ξ is reasonably assumed to be 0.2. In the following we study the relation between the avalanche size and avalanche duration in the context of a series of strain avalanche in micropillar plasticity. Specifically, we simulate the experimental strain-stress responses of the single nickel microcrystals having diameters between 10 μm and 30 μm at the nominal strain rates $\dot{\varepsilon}_0 = 1.0 \times 10^{-4}$.[1,5]

We verify the rationality of the present crystal plasticity model by comparing its predictions with the experimental observations with respect to the avalanche durations (at room temperature where more experimental data are available, as compared with the high temperature). Figure 2 shows the statistical distributions of the avalanche durations for ∼30 μm, ∼20 μm and ∼10 μm diameter samples. For those larger magnitudes of T_b (i.e., $T_\mathrm{b} \geq MS_\mathrm{min}/\dot{\varepsilon}_0$), they can be well characterized by a power-law behavior,

$$P(T_\mathrm{b}) \sim T_\mathrm{b}^{-\alpha} \exp[-(T_\mathrm{b}/T_0)^2], \tag{10}$$

which is truncated at a characteristic avalanche size T_0 due to finite size effects. According to Fig. 2, we find that the burst duration distributions $P(T_\mathrm{b})$ exhibit a robust power-law behavior with an exponent $\alpha = 1.65$ obtained by the maximum likelihood method.[20] This value is in line with a recent 3D analysis of experimental micropillar compression data.[13] Based on the estimated values of α, we fit the respective distribution function for the ∼30, ∼20 and ∼10 μm diameter samples to the data sets by choosing the appropriate values of T_0. For comparison, we also show the scaled experimental data from Ref. [5] wherein the micropillars (having diameters between 18 μm and 30 μm) were tested under the same loading conditions as we used in the simulations. The plot shows that the theoretically predicted collapse function falls on top of the experimental collapse. This reveals that our model not only predicts the scaling function but also predicts the exponents used for the successful collapse.

We now turn our attention to the relation between the avalanche duration and the avalanche size. Figure 3 shows the averaged avalanche size $\langle S\rangle$ as a function of the avalanche duration T_b. Across the grouped data sets, the averaged avalanche size scales with the avalanche duration as $\langle S\rangle \propto T_\mathrm{b}^{\gamma}$, with $\gamma = 0.80 \pm 0.01$. The plot clearly shows that the averaged avalanche size $\langle S\rangle$ scaling with T_b only holds for those larger magnitudes of avalanche durations. It is noted that the predicted scaling exponent γ is different from that derived by either the mean-field theory($\gamma = 2$)[23] or the discrete dislocation dynamic model ($\gamma = 1.32$).[12] Such a discrepancy partly arises from the selected scaling exponent of avalanche size, such as $\tau = 1.35$ in this study, rather than $\tau = 2$ obtained from the mean-field theory.[6] Despite this discrepancy, the present theoretical predictions are suggestive of the scaling behaviors shown from micro-compression tests,[5] discrete dislocation dynamic simulation[12] and the mean-field theory.[6]

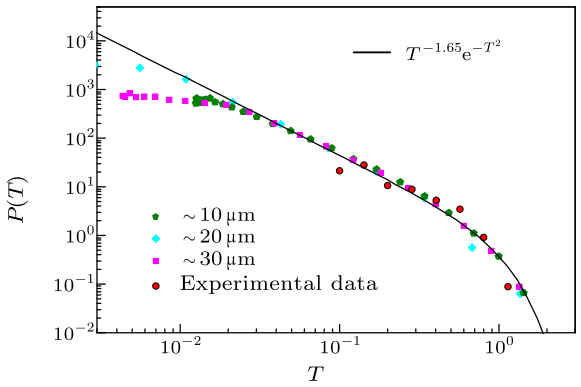

Fig. 2. Burst duration distributions for the Ni pillars of ∼10 μm, ∼20 μm and ∼30 μm diameters. The distributions are plotted as functions of $T = T_\mathrm{b}/T_0$. Note that y-axes of probability distributions are scaled from original dates, respectively. The lines represent the expression Eq. (10) that best fits to the corresponding simulation results. The best fitting values of T_0 for ∼10 μm, ∼20 μm and ∼30 μm diameter samples are 22.5 s, 15 s and 8 s, respectively. In the computations, we take $E = 221$ GPa, $\dot{\gamma}_0 = 1.0 \times 10^{-3}$/s, $M = 0.48$ for all the simulations. The hardening parameters (h_0, τ_0 and τ_s) in Eq. (4) have been discussed in Refs. [13,17]. Here we just show that the avalanche duration distributions derived from Eq. (8) agree with the experimental observations.[5]

We shall mention that the avalanche size S in Eq. (8) or Eq. (11), which follows a power law $S^{-\tau}$ as $\tau = 1.35$, serves as an input to calculate T_b in the present model. Accordingly, the calculated T_b follows Eq. (10) with the verification demonstrated by the collapse of all distributions for larger magnitudes of T_b (Fig. 2). Based on these two reasonable data sets (T_b and S), Fig. 3 plots the avalanche size S as a function of the avalanche duration T_b for the Ni pillars of ∼20 μm diameters. Although S is generally associated with the longer duration T_b, it is clear that S does not scale with T_b (see the inset of Fig. 3,). Instead we show that it is the averaged avalanche size $\langle S\rangle$ that scales with the avalanche duration.

To further understand why the avalanche size S does not scale with the avalanche duration T_b, we proceed to simplify Eq. (8) with a Taylor expansion. Neglecting the small terms of higher order, T_b can then be expressed as $T_\mathrm{b}(t,S) = \frac{S}{\dot{\gamma}^+(t)}[1+\alpha(t)S]$, where $\alpha(t) = \frac{\tau_\mathrm{in}(t)m}{h(t)\xi}$. According to our computations, we find $\alpha(t) \ll 1$ in the course of plastic flow. In this case, T_b can then be reasonably calculated by

$$T_\mathrm{b}(t,S) \approx S/\dot{\gamma}^+(t). \tag{11}$$

This equation is especially true when those avalanche sizes fall in the region of the pure power-law behavior, where the relative error between Eq. (11) and Eq. (8) is about 5% at most (i.e., less than 3% for the Ni pillars of ∼20 μm diameter). From Eq. (11), it is seen that T_b is determined by both the avalanche size S and the strain rate $\dot{\gamma}^+(t)$. In this case, T_b scaling as S may be not expected, due to the fact that the burst

strain rates are demonstrated to vary stochastically in a wide range of magnitudes, as the plastic deformation proceeds.[24]

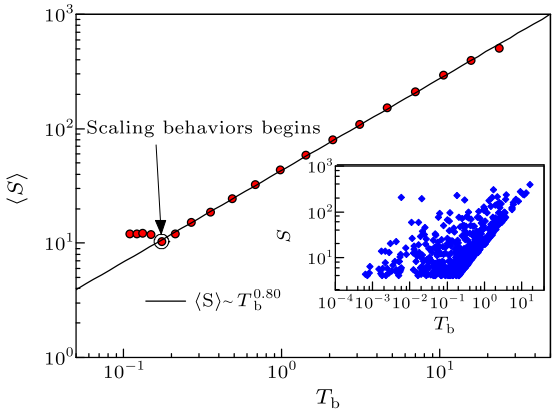

Fig. 3. Relation between the averaged avalanche size $\langle S\rangle$ and avalanche duration T_b from the simulations of the Ni pillars of ∼20 μm diameters. The straight line indicates a power-law scaling with a predicted exponent of 0.80±0.05, suggestive of the mean-field scaling.[7] For the collective date sets over a range of avalanche durations from ∼100 μs to ∼10 s, the scaling behavior is observed only for those larger avalanche durations (larger than 0.15 s). Inset: relation between the avalanche size S and avalanche duration T_b from the same date sets of the Ni pillars of ∼20 μm diameters.

One issue to be elucidated is that the present model was formulated within the framework of classic crystal plasticity.[16] Thus it is more suitable to investigate the characteristic sizes of micropillars larger than a few micrometers. In other words, the model are not applicable to the strain avalanche of pillars at submicron scale (100 nm–10 μm), since most shear slips that occur predominantly on the slip system with the highest Schmid factor may not be guaranteed. However, the present model can be further modified by incorporating the evolution of dislocation density into the slip resistance in Eq. (1). For example, the slip resistance in the present model can be alternatively derived by the SAD model in the term of dislocation density.[21] In this context, it may be valid for the modified model to study the strain avalanche of pillars at submicron scale.

In conclusion, the present work addresses the strain avalanche in the deformation of microsized single crystals. For the first time we provide the quantitative expression of the avalanche duration with respect to the avalanche size by a simple crystal plasticity model. The theoretical predictions clearly show that the avalanche duration scales with the averaged avalanche size, in agreement with experiments[5] and simulations.[12] However, we further suggest that such scaling behaviors only hold for those larger magnitudes of durations. It would be interesting to check these theoretical evidences on the basis of the direct measurements of strain avalanches possessing sufficiently high spatial resolution in the deforming microsized crystals.

References

[1] Dimiduk D M, Woodward C, LeSar R and Uchic M D 2006 *Science* **312** 1188
[2] Maaß R, Derlet P M and Greer J R 2015 *Small* **11** 341
[3] Maaß R Derlet P M and Greer J R 2015 *Phys. Rev.* E **91** 042403
[4] Csikor F F, Motz C, Weygand D, Zaiser M and Zapperi S 2007 *Science* **318** 251
[5] Papanikolaou S, Dimiduk D M, Choi W, Sethna J P, Uchic M D, Woodward C and Stefano Z 2012 *Nature* **490** 517
[6] Dahmen K A, Ben-Zion Y and Uhl J T 2009 *Phys. Rev. Lett.* **102** 175501
[7] Zhang X and Shang F L 2014 *Chin. Phys. Lett.* **31** 026401
[8] Ispánovity P D, Groma I, Györgyi G, Csikor F F and Weygand D 2010 *Phys. Rev. Lett.* **105** 085503
[9] Brinckmann S, Kim J Y and Greer J R 2008 *Phys. Rev. Lett.* **100** 155502
[10] Friedman N, Jennings A T, Tsekenis G, Kim J K, Tao M, Uhl J T, Greer J R and Dahmen K A 2012 *Phys. Rev. Lett.* **109** 095507
[11] Dimiduk D M, Nadgorny E M, Woodward C, Uchic M D and Shade P A 2010 *Philos. Mag.* **90** 3621
[12] Ispánovity P D, Laurson L, Zaiser M, Groma I, Zapperi S and Alava M J 2014 *Phys. Rev. Lett.* **112** 235501
[13] Zhang X, Shang F L, Yu Y, Yan Y B and Yan S P 2014 *Int. J. Solids Struct.* **51** 4519
[14] Ovaska M L, Laurson L and Alava M J 2015 *Sci. Rep-UK* **5** 10580
[15] Uchic M D and Dimiduk D M 2005 *Mater. Sci. Eng.* A **400** 268
[16] Peirce D, Asaro R J and Needleman A 1983 *Acta Met.* **31** 1951
[17] Zhang X and Shang F L 2014 *Int. J. Solids Struct.* **51** 1859
[18] Cui Y N, Lin P, Liu Z L and Zhuang Z 2014 *Int. J. Plast.* **55** 279
[19] Norfleet D M, Dimiduk D M, Polasik S J Uchic M D and Mills M J 2008 *Acta Mater.* **56** 2988
[20] Zhang X, Pan B and Shang F L 2012 *Europhys. Lett.* **100** 16005
[21] Lin P, Liu Z L, Cui Y N and Zhuang Z 2015 *Int. J. Solids Struct.* **69** 267
[22] Ng K S and Ngan N H W 2008 *Acta Mater.* **56** 1712
[23] Papanikolaou S, Bohn F, Sommer R L, Durin G, Zapperi S and Sethna J P 2011 *Nat. Phys.* **7** 316
[24] Ispánovity P D, Groma I, Györgyi G, Szabóet P and Hoffelner W 2011 *Phys. Rev. Lett.* **107** 085506